5 Applications

The development of QPCs has resulted in a wealth of experiments designed to investigate their fundamental properties and, in addition, has enabled many fascinating experiments associated with the properties of the material systems in which they are defined. However suggestions as to how these transport properties might be exploited for real device applications are to date somewhat meagre. Clearly, if the one-dimensionality of the channel itself is to be successfully exploited, clean systems with well defined subband energies in excess of $k_B T$ are required. Although high-temperature QPCs have been developed it is unlikely that room-temperature operation will be easily achieved in marked contrast to the situation in metallic point contact systems.

5.1 Transport applications

One device proposal to exploit the 1D transport properties relies upon the modulation of the velocity in the high-bias limit due to an increased optical-phonon scattering [92S4]. The energy dependence of the optical-phonon scattering diverges at the optical-phonon energy and is expected to decrease for energies in excess of this threshold value. This dependence can, in principle, be exploited to create a velocity-modulated field effect device in the 1D limit. In theory two distinct transport regions can be distinguished; velocity runaway for high electron densities and electron energies in excess of the optical-phonon energy, or so-called electron confinement where the kinetic energy along the channel is constrained to lie below the optical-phonon energy due to strong scattering. The latter is expected to occur in low-density 1D systems. This behaviour has been modelled using a time-dependent Boltzmann equation and the velocity modulation calculated. In conjunction with the expected excellent high-mobility in the linear-response limit this property could yield good device characteristics; in particular a high transconductance $g_m = \mathrm{d}I/\mathrm{d}V_\mathrm{g}$ and a high cut-off frequency for such field-effect transistors.

The application of a metallic QPC as an analog switching device has been successfully demonstrated in the low-frequency regime [95S2] by modulating the device conductance between the tunneling and quantized conductance states. In this experiment the conductance of a metallic QPC was tuned by adjusting the position of a nickel scanning tunneling microscope tip relative to a gold substrate. After an initial wetting of the nickel tip with gold atoms the conductance could be switched from an essentially zero conductance tunneling state to the first plateau, $0.977(2e^2/h)$, by modulating the tip position by roughly 2 Å, the switching itself occuring over a length scale of roughly 30 pm. A low-frequency signal ($\sim$ 1.4 kHz) applied to the nickel tip results in a device current which could be modulated via the piezoelectric signal used to tune the tip position. Although the switching speeds obtained via this method are comparatively slow, replacing the piezoelectric transducer with an appropriately micromachined electrostatic transducer should lead to better performance. In such metallic systems the current flows through an extremely narrow constriction ($\sim \lambda_\mathrm{F} \approx 5.2$ Å for Au) and it is suggested that the lateral extent of this essentially micromechanical switch is perhaps as small as a single gold atom.

A more sophisticated suggestion to exploit the conductance characteristics of ballistic QPCs lies in their use to realize elementary digital electronic functions [98C]. The basic building block for these electronic devices is a QPC with a tunable metallic island within the channel, which acts as a gate to modulate the width and hence the number of conducting modes of the device. Although this geometry is somewhat more complicated than a conventional split-gate QPC the fabrication of similar structures has been successfully demonstrated [95E, 97H2]. The application of a sinusoidal signal to the island-gate results in a comparable modulation of the channel width but in a digital variation of the channel conductance, as illustrated in Fig. 105. The output signal has the same frequency as the applied sine wave but the duty cycle depends upon both the initial island-gate width as well as the oscillation amplitude; this sensitivity of the device when operating as a digital clock to the inital signal amplitude provides additional discriminator functionality.

A parallel configuration of two such island-gate tuned QPCs can operate collectively as a

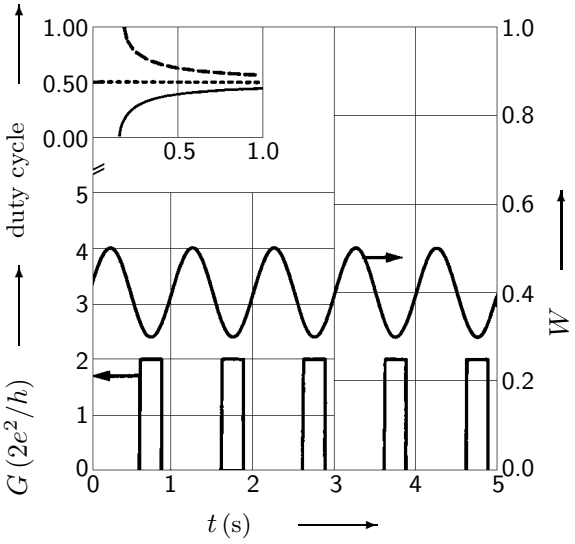

Fig. 105: Both the conductance G and the island width W are plotted as a function of time for a sinusoidal variation of the voltage applied to the island-gate. Also shown in the inset is the variation of the duty cycle as a function of the signal amplitude for three different initial widths [98C].

frequency doubler when identical but inverted sinusoidal inputs are applied to the two island-gates. Ideally, such operation requires a small amplitude sinusoidal signal operating close to the threshold value (i.e. with a duty cycle close to 0.25), which as can be seen from the inset in Fig. 105 might perform unreliably in a real device. Other suggestions for digital devices, based upon the technique discussed above, include hexadecimal counters for an identical set of devices fed with the appropriate frequency doubled signals.

5.2 High-frequency devices

Perhaps the most promising application for ballistic QPCs is to be found however not in their low-temperature conductance properties but rather in the non-linear current-voltage characteristics in the high-bias limit. In this limit, where $eV_{\mathrm{sd}} > E_{\mathrm{F}}$, the characteristics are essentially independent of the subband structure and as such relatively insensitive to temperature. The non-linearity occurs on a voltage scale comparable with the Fermi energy, which for typical semiconductor heterostructures is of the order of 10 meV. Beyond such energies the current-voltage characteristics tend to saturate and, in contrast with theoretical predictions, show no N-type negative differential conductance. Nevertheless, such characteristics are comparable with the those of SIS- (Superconducter-Insulator-Superconducter) mixer devices and can be expected to operate as sensitive mixers [94G1]. A single QPC operating in the non-linear regime can be expected to have a differential resistance of 10 kΩ and impedance matching the QPC to external sources presents a significant problem which was solved using discrete reactive components. The resulting mixing spectrum is illustrated in Fig. 106; the power levels of the individual mixing products are strongly modulated due to the fequency dependent impedance matching but an approximate binomial distribution can be seen for example for $2f_1, f_1 + f_2, 2f_2$ as expected. An optimal DC-bias point was not found due to device saturation but a clear correlation of the mixing signal with the applied gate-voltage could be determined as illustrated in Fig. 107. Presumably the maximum of the mixing signal represents the compromise between the increase of non-linearity as the QPC channel is defined and the increased device impedance, which leads to poorer impedance matching.

An improved broadband impedance matching can be obtained by integrating the number of active QPCs in a parallel device geometry [97H2]. Additional benefits are the increased power levels obtained in the mixing signals, and a decrease in parasitic source-drain capacitance resulting from the more effetive use of the substrate mesa. Such devices have been operated in the small-signal limit and the conversion loss of a typical device is shown in Fig. 108. Conversion losses as small as 13 dB have been obtained for low-tempearture operation, and successful device operation

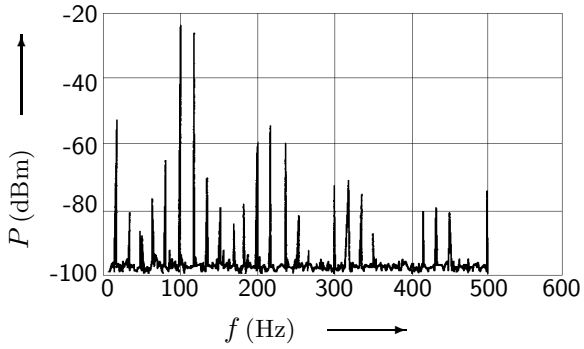

Fig. 106: The low-temperature mixing spectrum of an impedance matched QPC at a gate-voltage bias of $V_g = -900\,\mathrm{mV}$ corresponding to a conductance of $400\,\mu\mathrm{S}$, and roughly five occupied subbands [94G1].

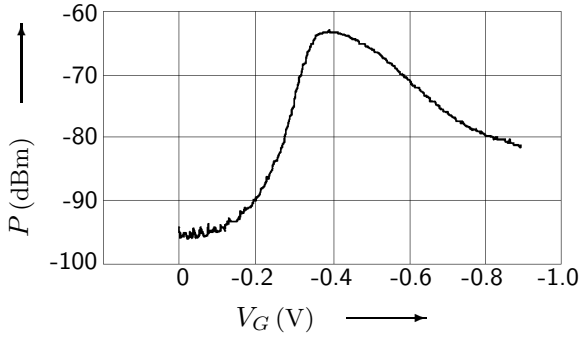

Fig. 107: The gate voltage dependence of the second order mixing product $f_1 - f_2$ with $f_1 = 356\,\mathrm{MHz}$ and $f_2 = 100\,\mathrm{MHz}$ [94G1].

at liquid nitrogen temperatures without significant degredation of device performance has been reported.

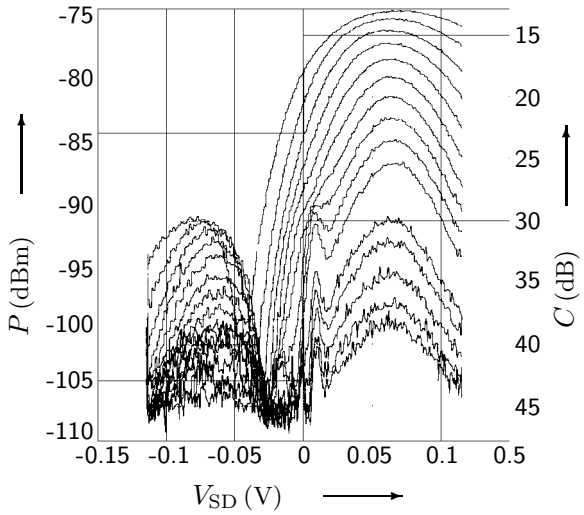

Fig. 108: The mixing power and the conversion loss for a parallel configuration of 155 QPCs is shown as a function of the applied source-drain bias for differing local oscillator power levels and for fixed gate voltage [97H2].

A most promising high-frequency device is the single electron current standard based upon the interaction of surface acoustic waves with QPCs [96S2]. The transport of charge in the potential minima of a SAW is modified by the lateral confinement produced by the QPC. The resultant quantized transmission of an integer number of electrons with each period of the radio frequency field leads to a quantized current $I = Nef_{\mathrm{rf}}$, where the driving frequency f_{rf} of the surface acoustic wave can be as large as several GHz. The number of transferred carriers is given by the number of discrete occupied states within the confining potential defined by the lateral quantization of the one-dimensional channel and the potential minima of the SAW. In the initial experiment the acoustoelectric current (see Fig. 109) was quantized with an accuracy of approximately 1 %, this figure being determined by the external experimental setup. The quantized steps are compara-

tively robust, however the observation of an accurate quantization requires the fine tuning of a large number of system parameters, in particular the gate-voltage and both the power level and frequency of the rf source. Despite the significantly larger current levels in such a device compared with the single-electron charge-pump the SAW device is unsuitable for metrological applications, nevertheless in individual samples an absolute accuracy of better than 0.15 % has been measured.

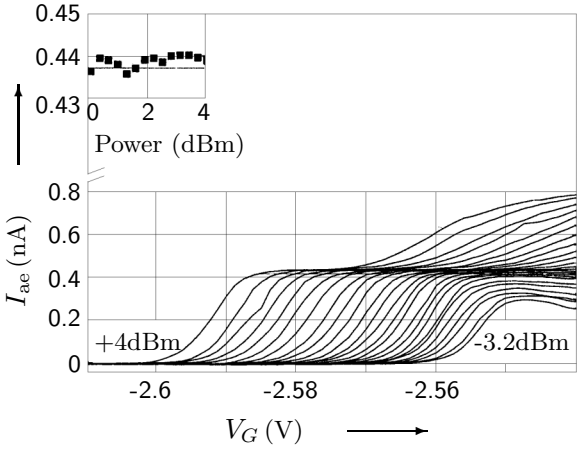

Fig. 109: The first conductance plateau in the acoustoelectric current for varying surface acoustic wave power [96S2]. The SAW frequency is 2728.6 MHz and the inset shows the plateau height as a function of applied rf power (the dotted line shows the quantized value $I = ef$).

5.3 References for Section 5

[92S4] Sone, J.: Semicond. Sci. Technol. **7** (1992) B210.

[94G1] Gödel, W., Manus, S., Wharam, D.A., Kotthaus, J.P., Böhm, G., Klein, W., Tränkle, G., Weimann, G.: Electron. Lett. **30** (1994) 977.

[95E] Eiles, T.M., Simmons, J.A., Sherwin, M.E., Klem, J.F.: Phys. Rev. B **52** (1995) 10756.

[95S2] Smith, D.P.E.: Science **269** (1995) 371.

[96S2] Shilton, J.M., Talyanskii, V.I., Pepper, M., Ritchie, D.A., Frost, J.E.F., Ford, C.J.B., Smith, C.G., Jones, G.A.C.: J. Phys.: Condens. Matter **L531** (1996) 8.

[97H2] Haubrich, A.G.C., Wharam, D.A., Kriegelstein, H., Manus, S., Lorke, A., Kotthaus, J.P., Gossard, A.C.: Appl. Phys. Lett. **70** (1997) 3251.

[98C] Cosby, R.M., Humm, D.R., Joe, Y.S.: J. Appl. Phys. **83** (1998) 3914.